



<b>Title</b>	<b>Modeling extreme values of processes observed at irregular time steps: application to significant wave height</b>
<b>Author(s)</b>	<b>Raillard, N; Ailliot, P; Yao, J</b>
<b>Citation</b>	<b>Annals of Applied Statistics, 2014, v. 8 n. 1, p. 1-647</b>
<b>Issued Date</b>	<b>2014</b>
<b>URL</b>	<b><a href="http://hdl.handle.net/10722/193216">http://hdl.handle.net/10722/193216</a></b>
<b>Rights</b>	<b>Creative Commons: Attribution 3.0 Hong Kong License</b>

# MODELING EXTREME VALUES OF PROCESSES OBSERVED AT IRREGULAR TIME STEPS: APPLICATION TO SIGNIFICANT WAVE HEIGHT

BY NICOLAS RAILLARD\*

*Laboratoire de Mathématiques de Bretagne Atlantique, UMR 6205, Université de Brest  
Laboratoire d'Océanographie Spatiale, IFREMER  
Insitutut de Recherche Mathématique de Rennes, UMR 6625, Université de Rennes 1*

BY PIERRE AILLIOT

*Laboratoire de Mathématiques de Bretagne Atlantique, UMR 6205, Université de Brest  
AND*

BY JIANFENG YAO

*Department of Statistics & Actuarial Sciences, The University of Hong Kong*

## *Abstract*

This work was motivated by the analysis of the extremal behavior of buoy and satellite data describing wave conditions in the North Atlantic Ocean. The available datasets consist of time series of significant wave height (Hs) with irregular time sampling. In such a situation, the usual statistical methods available for analyzing extreme values cannot be used directly. The method proposed in this paper is an extension of the peaks over threshold (POT) method, where the distribution of a process above a high threshold is approximated by a max-stable process whose parameters are estimated by maximizing a composite likelihood function. The efficiency of the proposed method is assessed on an extensive set of simulated data. It is shown, in particular, that the method is able to describe the extremal behavior of several common time series models with regular or irregular time sampling. The method is then used to analyze Hs data in the North Atlantic Ocean. The results indicate that it is possible to derive realistic estimates of the extremal properties of Hs from satellite data despite its complex space-time sampling.

**1. Introduction.** Extreme events are a major concern in statistical modeling and appropriate statistical methods are needed to derive estimations of the extremal properties of various phenomena from complex observations. For example, the 100-year return level of significant wave height is often used in the design of marine structures as a criterion to

---

\*Corresponding Author (E-mail: nicolas.raillard@gmail.com)

*Keywords and phrases:* Extreme values, time series, max-stable process, composite likelihood, irregular time sampling, significant wave height, satellite data.

characterize the extreme waves that a structure may face during its lifetime. Significant wave height, generally denoted  $H_s$ , can be interpreted as a measure of an average wave height in a sea state. Three main sources of data can be used to assess the statistical properties of  $H_s$ :

- *Reanalysis data* provide long time series (typically a few decades) everywhere in the oceans at a regular time step and without missing values, but tend to smooth out extreme values.
- *Buoy data* are generally more accurate, but cover shorter time periods (typically a few years with missing values) and have a poor spatial distribution.
- *Satellite data* are also accurate observations and are available on the last 20 years. However, the time series obtained by selecting all satellite data available at a given location exhibits complex irregular time sampling depending on the number and tracks of the operating satellites.

A typical example of the data coverage over a 24-hour time window in the North Atlantic is given in Figure 1. The motivation for the work presented here was to develop statistical methods for analyzing the extremal properties of  $H_s$  based on such datasets. In particular, our proposed method can be used to estimate various characteristics of the extremal behavior of processes (e.g. high quantiles, return periods, storm durations, etc.) observed at regular or irregular time steps, whereas most existing methods are inappropriate in the latter case.

Two methods are commonly used for estimating extreme quantiles (see e.g. Embrechts, Klüppelberg and Mikosch (1997), Coles (2001); Beirlant et al. (2004); de Haan and Ferreira (2006), and the references therein). The first one, generally referred as the block maxima method, relies on probabilistic results, which suggest the use of the generalized extreme-value (GEV) distribution for modeling the maximum of a large number of identically distributed random variables. The main drawback of this approach is the waste of data induced by taking the maximum over a large block, typically one year for meteorological applications, before fitting the GEV distribution. The second approach, generally referred to as peaks over threshold (POT), involves keeping only the observations above a certain threshold chosen to be sufficiently high to ensure that the distribution of excesses above that threshold is well approximated by a generalized Pareto distribution (GPD). A problem that arises in using the POT approach for time series is that clusters of consecutive dependent exceedances are generally observed, particularly when the time-lag between successive observations is smaller than the characteristic duration of extreme events. In this case a "declustering" step is generally applied before fitting the GPD distribution to the sample of cluster maxima. This method also leads to waste data since only one value per cluster is kept to fit the GPD, and it relies on arbitrary rules for declustering the data. Those rules are even more difficult to choose in the presence of missing values or irregular time sampling.

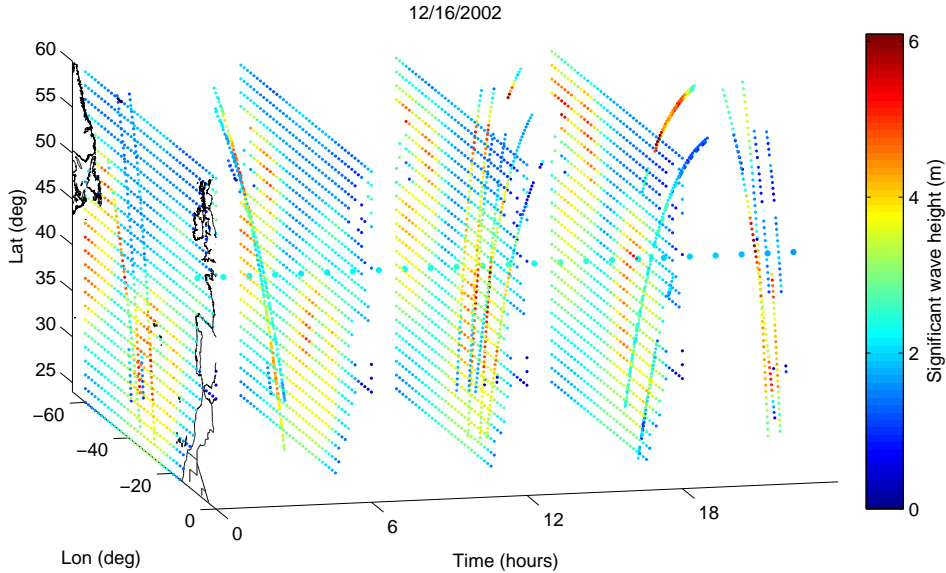


FIGURE 1. 3D representation of the available data for 12/16/2002. The 2D fields at times 0, 6, 12 and 18 correspond to reanalysis data, the 24 observations at the same location correspond to buoy data (hourly data), and the other data to the various satellite tracks.

Another approach, initially proposed in [Smith, Tawn and Coles \(1997\)](#), retains all of the exceedances and models them as a first-order Markov chain whose transition kernel is derived from bivariate extreme value theory. A concurrent strategy, adopted for example in [Bortot and Gaetan \(2013\)](#), consists of modeling the exceedances conditionally on a latent process. Both approaches have been successfully applied to various meteorological time series (see e.g. [Ribatet et al. \(2009\)](#)), but they cannot be adapted straightforwardly to time series with irregular sampling (see also [Reich, Shaby and Cooley \(2013\)](#)). In this paper, we propose an alternative approach in which the time series of exceedances above a high threshold is assumed to be a realization of a censored max-stable process. This model is motivated by probabilistic results from extreme value theory. Since the full likelihood cannot be obtained analytically, we follow recent works on spatial and space-time extremes, and base the statistical inference on a composite likelihood approach. The proposed model can be easily simulated, thereby allowing estimation of various quantities of interest for the applications, such as quantiles, return periods or the characteristics of sojourns above high thresholds using Monte-Carlo simulations. Parametric bootstrap can also be used to assess the accuracy of the estimators.

The model is introduced in [Section 2](#). [Section 3](#) introduces the composite likelihood approach and discusses the properties of the estimators using simulations. [Section 4](#) describes simulation results to validate our approach on classical time-series models and [Section 5](#)

discusses its application to Hs data.

## 2. Censored max-stable process.

2.1. *Threshold models and censoring in the independent case.* Probably the most classical approach to modeling the extremal properties of an independent and identically distributed (iid) sample  $(X_1, \dots, X_n)$  consists in using the "block maxima" approach. It relies on the probabilistic results originating in [Fisher and Tippett \(1928\)](#) which suggest approximating the distribution of  $M_n = \max_{i=1, \dots, n} X_i$  by a GEV distribution with the following cumulative distribution function (cdf):

$$(1) \quad F(x; \mu, \sigma, \xi) = \begin{cases} \exp\{-[1 + \xi \frac{x-\mu}{\sigma}]^{-\frac{1}{\xi}}\} & (\xi \neq 0) \\ \exp\{-\exp[-\frac{x-\mu}{\sigma}]\} & (\xi = 0) \end{cases},$$

defined for  $x$  such that  $(1 + \xi \frac{x-\mu}{\sigma}) > 0$  with parameters  $\mu \in \mathbb{R}$ ,  $\sigma > 0$ , and  $\xi \in \mathbb{R}$ . For practical applications, the data are grouped into blocks of equal length, and a GEV distribution is fitted to the sample of block maxima. The choice of block size is critical in practice. For environmental time series, the GEV distribution is generally fitted to the time series of annual maxima to remove seasonal effects. This leads to an important waste of data, and the sample size used to estimate the three parameters of the GEV distribution is the number of years with no or few missing values (a few decades in the best-case scenario). Although many methods have been proposed in the literature to provide estimates which exhibit a good behavior on small samples (see e.g. [Ailliot, Thompson and Thomson \(2011\)](#) and references therein), such estimation remains an important issue in practical applications.

The POT approach is the classical alternative to the block maxima approach. It is less wasteful of data since it keeps all data above a high threshold  $u$  which is chosen such that the conditional distribution  $\mathbb{P}[X_i \leq x | X_i > u]$  is well approximated by a GPD with cdf

$$G(x; \mu, \sigma, \xi) = \begin{cases} 1 - \left(1 + \xi \frac{x-\mu}{\sigma}\right)^{-1/\xi} & (\xi \neq 0), \\ 1 - \exp[-\frac{x-\mu}{\sigma}] & (\xi = 0), \end{cases}$$

defined for  $x \geq \mu$  such that  $(1 + \xi \frac{x-\mu}{\sigma}) \geq 0$  with  $\mu = u$  and parameters  $\sigma > 0$  and  $\xi \in \mathbb{R}$ . Again, the use of the GPD is motivated by probabilistic results, and various methods have been proposed in the literature for estimating the two parameters of the GPD based on the sample of exceedances and the choice of  $u$ , although the latter is a more difficult problem to handle (see [Davison and Smith \(1990\)](#)). Once  $u$  is chosen, the standard method for

estimating the unknown parameters is to maximize the likelihood function

$$\begin{aligned}
 L(\lambda, \sigma, \xi; X_1, \dots, X_n) &= \lambda^{N_u} (1 - \lambda)^{n - N_u} \prod_{i \in \{1, \dots, n\} | X_i > u} g(x_i; u, \sigma, \xi) \\
 (2) \qquad \qquad \qquad &= \prod_{i \in \{1, \dots, n\} | X_i \leq u} \lambda \prod_{i \in \{1, \dots, n\} | X_i > u} (1 - \lambda) g(x_i; u, \sigma, \xi),
 \end{aligned}$$

where  $\lambda = \mathbb{P}(X_i \leq u)$ ,  $N_u$  is the number of observations below the threshold  $u$ , and  $g(x; \mu, \sigma, \xi)$  is the probability density function (pdf) of the GPD. It is well known that the conditional distribution of the exceedances of a GPD above an arbitrary threshold is also a GPD, which allows us to interpret (2) as the likelihood of an iid sample of a GPD censored at the threshold  $u$ . More precisely, let  $(\tilde{X}_1, \tilde{X}_2, \dots, \tilde{X}_n)$  be an iid sample of a GPD with parameter  $(\mu, \tilde{\sigma}, \xi)$ , and consider the censored random variable

$$Y_i = u \mathbb{1}_{[\tilde{X}_i \leq u]} + \tilde{X}_i \mathbb{1}_{[\tilde{X}_i > u]} = \begin{cases} u & \text{if } \tilde{X}_i \leq u, \\ \tilde{X}_i & \text{if } \tilde{X}_i > u, \end{cases}$$

where the threshold  $u$  belongs to the support of the GPD distribution. We have  $P(Y_i = u) = \lambda$  with  $\lambda = G(u; \mu, \tilde{\sigma}, \xi)$  and, for  $x > u$ ,

$$\begin{aligned}
 \mathbb{P}(Y_i \geq x) &= \mathbb{P}(\tilde{X}_i \geq u) \mathbb{P}(\tilde{X}_i \geq x | \tilde{X}_i \geq u) \\
 &= (1 - G(u; \mu, \tilde{\sigma}, \xi)) \frac{1 - G(x; \mu, \tilde{\sigma}, \xi)}{1 - G(u; \mu, \tilde{\sigma}, \xi)} \\
 &= (1 - \lambda)(1 - G(x; u, \sigma, \xi)),
 \end{aligned}$$

with  $\sigma = \tilde{\sigma} \left(1 + \xi \frac{u - \mu}{\tilde{\sigma}}\right)$ , and thus (2) is the likelihood of  $(Y_1, \dots, Y_n)$ . Finally, the assumptions made when using the POT approach are equivalent to assuming that the original sample  $(X_1, \dots, X_n)$  satisfies

$$(3) \qquad \qquad \qquad u \mathbb{1}_{[X_i \leq u]} + X_i \mathbb{1}_{[X_i > u]} = u \mathbb{1}_{[\tilde{X}_i \leq u]} + \tilde{X}_i \mathbb{1}_{[\tilde{X}_i > u]},$$

for all  $i \in \{1, \dots, n\}$ , where  $(\tilde{X}_1, \dots, \tilde{X}_n)$  is an iid sample of a GPD.

We will see below that this interpretation of the POT approach in terms of censoring has certain advantages for modeling purposes. From a numerical point of view, it can be viewed as a reparametrization of the likelihood function. Maximizing (2) over  $(\lambda, \sigma, \xi)$  leads to the following estimate for  $\lambda$ ,  $\hat{\lambda} = \frac{N_u}{n}$  which has the desirable properties of being easy to interpret and of being independent of the estimates of  $\sigma$  and  $\xi$ . At the same time, maximizing (2) over  $(\mu, \tilde{\sigma}, \xi)$  leads to a more complicated three-dimensional optimization problem and correlated estimates, which can be problematic for certain applications as discussed in Section 5 and in Ribereau, Naveau and Guillou (2011).

Although the GPD distribution is the most common choice for modeling exceedances over a high threshold, other tail approximations have been proposed in the literature. In particular, we have

$$G(x; \mu, \sigma, \xi) \approx F(x; \mu, \sigma, \xi)$$

for "high" values of  $x$  (see [Drees, de Haan L. and Li \(2006\)](#)) and this suggests that similar results will be obtained if we model the distribution of  $\tilde{X}_i$  by a GEV distribution instead of a GPD. Various tests on simulated samples have confirmed that both approximations lead to similar results in practice.

The tail approximations discussed above remain valid for dependent sequences under mild conditions (see [Leadbetter, Lindgren and Rootzén \(1983\)](#)) which justifies the use of both the block maxima and POT approaches for analyzing the extremes of time series. One difficulty with using the POT approach in this context is that clusters of consecutive dependent exceedances are generally observed, whereas the likelihood function (2) is the joint distribution of the exceedances only if they are independent. The most common POT method thus includes a declustering step, with the maxima within each cluster kept only to obtain a sample of approximately independent exceedances. It also leads to waste data and thus degrades the quality of the estimates. Alternative strategies, which keep all the exceedances in the fitting procedure but correct the estimation of the uncertainty of the estimators to account for dependence, are proposed in [Fawcett and Walshaw \(2007, 2012\)](#).

*2.2. Censored max-stable process.* We now consider a sample  $(X_{t_1}, \dots, X_{t_n})$  of a stochastic process  $\{X_t\}$  observed at time  $(t_1, \dots, t_n)$ . It is generally assumed in the literature that the observations are available at a regular time step (i.e.  $t_{i+1} - t_i = t_{j+1} - t_j$  for all  $(i, j) \in \{1, \dots, n-1\}$ ), but we are interested in a method that is sufficiently flexible to deal with irregular time sampling. We thus propose analyzing the extremal behavior of such a dataset by extending the POT approach and modeling the exceedances of the process  $\{X_t\}$  above a high threshold  $u$  as a censored max-stable process. The theory of max-stable processes (see [de Haan \(1984\)](#); [de Haan and Ferreira \(2006\)](#)) is a natural generalization of the traditional univariate max-stable theory used to motivate the choice of the GEV distribution in the iid case. Several families of max-stable processes have been proposed in the literature (see e.g. [Smith \(1990\)](#); [Schlather \(2002\)](#)). Our focus here is on the specific *Gaussian extreme value process* introduced in [Smith \(1990\)](#) although the methodology introduced herein can easily be adapted to other models. More precisely, we assume that

$$(4) \quad u\mathbb{1}_{[X_t \leq u]} + X_t\mathbb{1}_{[X_t > u]} = u\mathbb{1}_{[\tilde{X}_t \leq u]} + \tilde{X}_t\mathbb{1}_{[\tilde{X}_t > u]}$$

holds for all  $t$ , where  $u$  is a fixed threshold and  $\{\tilde{X}_t\}$  is a stationary Gaussian extreme value process with parameter  $\theta = (\mu, \sigma, \xi, \nu) \in (-\infty, +\infty) \times (0, +\infty) \times (-\infty, +\infty) \times (0, +\infty)$ , as defined below.

- The marginal distribution of  $\{\tilde{X}_t\}$  is a GEV distribution with parameter  $(\mu, \sigma, \xi)$ . This assumption implies that the process  $\{Z_t\}$  obtained by applying the following marginal transformation

$$(5) \quad Z_t = -\frac{1}{\log(F(\tilde{X}_t; \mu, \sigma, \xi))}$$

is a stationary process with a unit Fréchet marginal distribution (i.e. GEV distribution with parameter  $(1, 1, 1)$ ).

- We further assume that

$$(6) \quad Z_t = \max \left\{ \frac{\zeta_i}{\nu\sqrt{2\pi}} \exp \left( -\frac{(s_i - t)^2}{2\nu^2} \right) \right\},$$

where  $\{(\zeta_i, s_i), i \geq 1\}$  denote the points of a Poisson process on  $(0, \infty) \times \mathbb{R}$  with intensity measure  $\zeta^{-2}d\zeta \times ds$ .

We focus on Gaussian extreme value processes because they have a nice meteorological interpretation (see [Smith \(1990\)](#)), can easily handle observations available at irregular time steps and are quick and easy to simulate (see [Schlather \(2002\)](#)). The following sections also show that these processes provide a flexible class of models which is able to describe the extremal behavior of most standard time series models and the Hs data considered in this work. Parameters  $\mu$ ,  $\sigma$  and  $\xi$  are related to the marginal distribution and can be interpreted, respectively, as location, scale and shape parameters, whereas parameter  $\nu$  is related to the temporal structure of the process and may be interpreted as the typical duration of storms. More precisely, we have (see [Smith \(1990\)](#)):

$$(7) \quad \mathbb{P}(Z_{t_1} \leq z_{t_1}, Z_{t_2} \leq z_{t_2}) = F_Z(z_{t_1}, z_{t_2}; \nu) = \exp[-V(z_{t_1}, z_{t_2}; \nu)],$$

where

$$(8) \quad V(z_{t_1}, z_{t_2}; \nu) = \frac{1}{z_{t_1}} \Phi \left( \frac{a}{2} + \frac{1}{a} \log \frac{z_{t_2}}{z_{t_1}} \right) + \frac{1}{z_{t_2}} \Phi \left( \frac{a}{2} + \frac{1}{a} \log \frac{z_{t_1}}{z_{t_2}} \right),$$

with  $a = \frac{|t_1 - t_2|}{\nu}$ , and  $\Phi$  is the cdf of the standard normal distribution. The limit cases  $\nu \rightarrow 0$  and  $\nu \rightarrow +\infty$  correspond to independence and perfect dependence, respectively.

Applying the inverse marginal transformation leads to the following bivariate cdf for the Gaussian extreme value process  $\{\tilde{X}_t\}$ :

$$(9) \quad \begin{aligned} F_{\tilde{X}}(\tilde{x}_{t_1}, \tilde{x}_{t_2}; \theta) &= \mathbb{P}(\tilde{X}_{t_1} \leq \tilde{x}_{t_1}, \tilde{X}_{t_2} \leq \tilde{x}_{t_2}) \\ &= \exp \left[ -\frac{1}{z_{t_1}} \Phi \left( \frac{a}{2} + \frac{1}{a} \log \frac{z_{t_2}}{z_{t_1}} \right) - \frac{1}{z_{t_2}} \Phi \left( \frac{a}{2} + \frac{1}{a} \log \frac{z_{t_1}}{z_{t_2}} \right) \right], \end{aligned}$$

with  $z_{t_i} = \frac{-1}{\log F(\tilde{x}_{t_i}; \mu, \sigma, \xi)}$ .

The bivariate distribution of  $(Y_{t_1}, Y_{t_2})$ , where  $Y_t = u\mathbb{1}_{[\tilde{X}_t \leq u]} + \tilde{X}_t\mathbb{1}_{[\tilde{X}_t > u]}$  is the censored Gaussian extreme value process, has the following bivariate pdf:

$$(10) \quad p_Y(y_{t_1}, y_{t_2}; \theta) = \begin{cases} F_{\tilde{X}}(u, u; \theta), & \text{if } y_{t_1} = u \text{ and } y_{t_2} = u, \\ \frac{\partial F_{\tilde{X}}}{\partial \tilde{x}_{t_1}}(y_{t_1}, u; \theta), & \text{if } y_{t_1} > u \text{ and } y_{t_2} = u, \\ \frac{\partial F_{\tilde{X}}}{\partial \tilde{x}_{t_2}}(u, y_{t_2}; \theta), & \text{if } y_{t_1} = u \text{ and } y_{t_2} > u, \\ \frac{\partial^2 F_{\tilde{X}}}{\partial \tilde{x}_{t_1} \partial \tilde{x}_{t_2}}(y_{t_1}, y_{t_2}; \theta), & \text{if } y_{t_1} > u \text{ and } y_{t_2} > u, \end{cases}$$



with respect to the product measure  $m \otimes m$ , where  $m(dx) = \delta_u(dx) + dx$  is the measure obtained by mixing the Dirac measure at  $u$  with the Lebesgue measure.

Similar approximations, motivated by probabilistic results from bivariate extreme value theory, are used in [Smith, Tawn and Coles \(1997\)](#) and [Ribatet et al. \(2009\)](#) to model the bivariate distribution of successive exceedances. Those papers further assume that the censored process is a Markov process and the full likelihood function is derived from the bivariate distributions. More recently, threshold versions of max-stable processes were also proposed in a space-time context (see [Huser and Davison \(In press\)](#); [Jeon and Smith \(2012\)](#)).

### 3. Parameter estimation.

3.1. *Composite likelihood estimators.* In this section,  $(y_{t_1}, \dots, y_{t_n}) \in (u, +\infty)^n$  denotes a realization of a Gaussian extreme value process  $\{Y_t\}$  with unknown parameter  $\theta^* = (\mu^*, \sigma^*, \xi^*, \nu^*)$  censored at the threshold  $u \geq 0$  and observed at time  $(t_1, \dots, t_n)$ . There is no known tractable expression for the full likelihood. However, since the marginal and bivariate distributions have tractable expressions, the statistical inference can be based on one of the composite likelihood functions introduced below (see also [Lindsay \(1988\)](#); [Varin and Vidoni \(2005\)](#); [Varin \(2008\)](#); [Cox \(2004\)](#); [Padoan, Ribatet and Sisson \(2010\)](#)).

- The *independent likelihood* function is defined as

$$(11) \quad IL(\theta; y_{t_1}, \dots, y_{t_n}) = \prod_{i=1}^n p_Y(y_{t_i}; \theta),$$

where  $p_Y(y_t; \theta)$  is the pdf of the marginal distribution of  $Y_t$  with respect to measure  $m$ . It is given by

$$p_Y(y_t; \theta) = \begin{cases} F(u; \mu, \sigma, \xi), & \text{if } y_t = u, \\ f(y_t; \mu, \sigma, \xi), & \text{if } y_t > u, \end{cases}$$

where  $F$  and  $f$  denote the cdf and pdf of the GEV distribution, respectively. It corresponds to the likelihood function of an iid sample of a censored GEV distribution (see [Section 2.1](#)) and does not depend on parameter  $\nu$ , which describes the dependence structure of the process. We denote by MILE the estimator of  $(\mu, \sigma, \xi)$  obtained by maximizing this function.

- The *pairwise likelihood* function

$$(12) \quad PL(\theta; y_{t_1}, \dots, y_{t_n}) = \prod_{i=1}^{n-1} \prod_{j>i} p_Y(y_{t_i}, y_{t_j}; \theta)^{\omega_{t_i, t_j}},$$

with  $p_Y(y_{t_i}, y_{t_j}; \theta)$  given by [\(10\)](#) and  $\omega_{t_i, t_j} \in \{0, 1\}$  indicates whether the pair of observations  $(y_{t_i}, y_{t_j})$  contributes to the pairwise likelihood function. This approach

has already been considered for time series with regular time sampling (see [Varin \(2008\)](#) and the references therein). It is generally assumed that

$$(13) \quad \omega_{t_i, t_j} = \mathbb{1}_{[|i-j| \leq K]},$$

such that only the pairs of observations less than  $K$  time units apart are retained to build the pairwise likelihood function. Hereafter,  $PL_K$  denotes the corresponding pairwise likelihood function and  $MPL_{KE}$  the estimator obtained by maximizing this function. Retaining only the neighboring observations (i.e. using  $K = 1$ ) has clear computational benefits since it permits to significantly reduce the number of terms in the product (12). It may also lead to more efficient estimators in practice (see [Varin \(2008\)](#) and [Section 3.2](#)). Another strategy is to retain the pairs of observations separated by a time lag smaller than  $K$  and take

$$(14) \quad \omega_{t_i, t_j} = \mathbb{1}_{[|t_i - t_j| \leq K]}.$$

This second strategy is similar to the first one when the process is observed at regular time sampling but differs in the irregular case, which will be further discussed using simulations in [Section 3.2](#).

- The *Markovian likelihood* function is defined as

$$(15) \quad \begin{aligned} ML(\theta; y_{t_1}, \dots, y_{t_n}) &= p_Y(y_{t_1}; \theta) \prod_{i=2}^n p_Y(y_{t_i} | y_{t_{i-1}}; \theta) \\ &= \frac{\prod_{i=2}^n p_Y(y_{t_i}, y_{t_{i-1}}; \theta)}{\prod_{i=2}^{n-1} p_Y(y_{t_i}; \theta)} \\ &= \frac{PL_1(\theta; y_{t_1}, \dots, y_{t_n})}{IL(\theta; y_{t_2}, \dots, y_{t_{n-1}})}, \end{aligned}$$

and MMLE denotes the estimator obtained by maximizing this function. This estimator is considered for comparison purposes. Indeed, when the process is observed at a regular time step, we retrieve the Markovian model considered in [Smith, Tawn and Coles \(1997\)](#) and [Ribatet et al. \(2009\)](#) for the specific bivariate max-stable distribution associated with the Gaussian extreme value process.

From a numerical point of view, we find it useful to use a two-stage procedure, where the parameters  $(\mu, \sigma, \xi)$  of the marginal distribution are first estimated by maximizing the independent likelihood function, and the dependence parameter  $\nu$  is then estimated by maximizing the pairwise likelihood function in  $\nu$  with the parameters of the marginal distribution kept fixed to the values obtained in the first step. Doing so permits us to reduce the computational time (the independent likelihood function can be evaluated quickly compared to the pairwise likelihood function) and avoid the divergence problems which may occur when optimizing the pairwise likelihood function simultaneously over all parameters

with an inappropriate starting point. Then, we can perform a global optimization of the pairwise likelihood function over the four parameters with the estimates obtained after the two-stage procedure being used as the starting point. We performed various numerical experiments, which confirmed that the estimators obtained from the two-stage procedure are suboptimal compared to full optimization (see [dos Santos and Lopes \(2008\)](#) for a discussion in the context of copulas).

The asymptotic properties of the composite likelihood estimators for max-stable processes have been studied in several recent papers. In [Padoan, Ribatet and Sisson \(2010\)](#) it is shown that they are consistent and asymptotically normal when the sample consists of iid replicates of max-stable fields. Two recent papers ([Huser and Davison \(In press\)](#); [Jeon and Smith \(2012\)](#)) consider the general case of temporally and spatially dependent max-stable processes. Although the asymptotic results developed in [Jeon and Smith \(2012\)](#) apply to the estimators considered in this paper, for the sake of completeness, an alternative proof of the consistency of the  $\text{MPL}_1\text{E}$  is provided in the supplementary article [Raillard, Ailliot and Yao \(2013\)](#). That proof is provided in an idealized situation with no censoring and known marginal distributions. Moreover, since the asymptotic covariance of the estimator is too complicated to compute for practical applications, we use parametric bootstrap (see e.g. [Benton and Krishnamoorthy \(2002\)](#)) to approximate the distribution of the estimators and provide confidence intervals, as discussed in greater details in Section 5.

*3.2. Simulation study.* A simulation study was undertaken to assess the accuracy of the estimators introduced in Section 3.1. Random samples were generated from a Gaussian extreme value process with parameters  $\mu = 0$ ,  $\sigma = 1$  and  $\xi = 0.3$ , which correspond to realistic values for environmental applications. We performed various experiments to investigate how the accuracy of the estimators is affected by sample size  $n$ , dependence parameter  $\nu$ , the threshold  $u$ , and, finally, by the strategy used to select the pairs of observations that contribute to the pairwise likelihood function. For each experiment, 1000 independent sequences of a Gaussian extreme value process were generated, and the various estimators of  $(\mu, \sigma, \xi, \nu)$  computed for each sequence.

Let us first focus on the case in which the time step between successive observations is constant. According to the left plots of Figure 2, all of the estimators seem to be consistent. We also checked empirically that, when multiplied by  $\sqrt{n}$ , the errors are almost constant, demonstrating that we retrieve the usual speed of convergence. The MLE is clearly the least efficient estimator, whereas the  $\text{MPL}_1\text{E}$ ,  $\text{MPL}_5\text{E}$  and MMLE produce similar results. A closer look reveals, however, that the  $\text{MPL}_5\text{E}$  is the least accurate of these three estimators. The MMLE slightly outperforms the  $\text{MPL}_1\text{E}$  in estimating scale parameter  $\sigma$  and shape parameter  $\xi$  whereas the  $\text{MPL}_1\text{E}$  provides the best estimator of dependence parameter  $\nu$ . The second column of Figure 2 shows that the root-mean-square error (RMSE) of all the estimators decreases with dependence parameter  $\nu$  and that it is more difficult to obtain reliable estimates when the dependence between successive observations is strong. The efficiency of the MMLE generally deteriorates quicker when  $\nu$  increases. It provides

the worst estimation of  $\mu$ ,  $\sigma$  and  $\nu$  when  $\nu \geq 1$  but provides the best estimation of  $\xi$  for all the values of  $\nu$  considered in this experiment. These results indicate that the Markovian likelihood may not be appropriate when the dependence is strong. The third column of Figure 2 depicts the behavior of the different estimators when censoring occurs. As expected, they all worsen when the threshold increases and the number of non-censored observations decreases. It can be seen that the estimator which suffers most from censoring is the MILE, whereas the MMLE outperforms both the  $\text{MPL}_1\text{E}$  and  $\text{MPL}_5\text{E}$  in estimating the parameters of the marginal distribution. The  $\text{MPL}_1\text{E}$  again provides the best estimator of the dependence parameter  $\nu$ .

The last column of Figure 2 shows the influence of the windows considered in defining the neighborhood, which are taken into account in the pairwise likelihood functions. The Gaussian extreme value process was simulated using an irregular time sampling (the time lag between successive observations was drawn from a uniform distribution on  $[0, 2]$ ) to allow comparison between the two strategies discussed in Section 3.1: the first involves the use of the  $K$  closest observations (see Equation (13)), whereas the second takes into account all observations falling within  $K$  time steps (see Equation (14)). We found the first strategy always to be the best. The evolution of RMSE with  $K$  differs according to the strategy used. It is increasing for the first strategy, meaning that the best estimators are obtained with  $K = 1$ , but generally decreasing for the second and the difference between both strategies decreases when  $K$  increases. Comparison with the MILE and MMLE indicates again that even when the time sampling is irregular the MMLE slightly outperforms the  $\text{MPL}_1\text{E}$  in estimating  $\mu$ ,  $\sigma$  and  $\xi$  but the  $\text{MPL}_1\text{E}$  provides the best estimation of  $\nu$ .

The results given in this section suggest that the MMLE or  $\text{MPL}_1\text{E}$  are more favorable for practical applications since their RMSE are generally the lowest. The two estimators have a similar computational cost. Although the former may provide a slightly better estimation when the dependence between successive observations is small, it is clearly less efficient when the dependence is strong. Finally, it seems reasonable to use the  $\text{MPL}_1\text{E}$  in practical applications and we will mainly focus on this estimator in the sequel.

**4. Performance on classical time series models.** The lack of data makes it generally difficult to validate models for extreme values when facing real applications. In this section, we perform a simulation study to check whether the proposed methodology is able to capture the extremal properties of several widely used time series models. In Section 4.1, we simulate large samples to obtain estimators with a low variance and to check whether the Gaussian extreme value process provides an appropriate approximation of the extremal behavior of the time series models under consideration. Then, in Section 4.2, we simulate shorter time series to validate the overall methodology in a more realistic context for practical applications.

4.1. *Model validation.* We focus on the following time series models:

- **IID:**  $\{X_t\}$  is an iid sequence of a standard normal distribution.

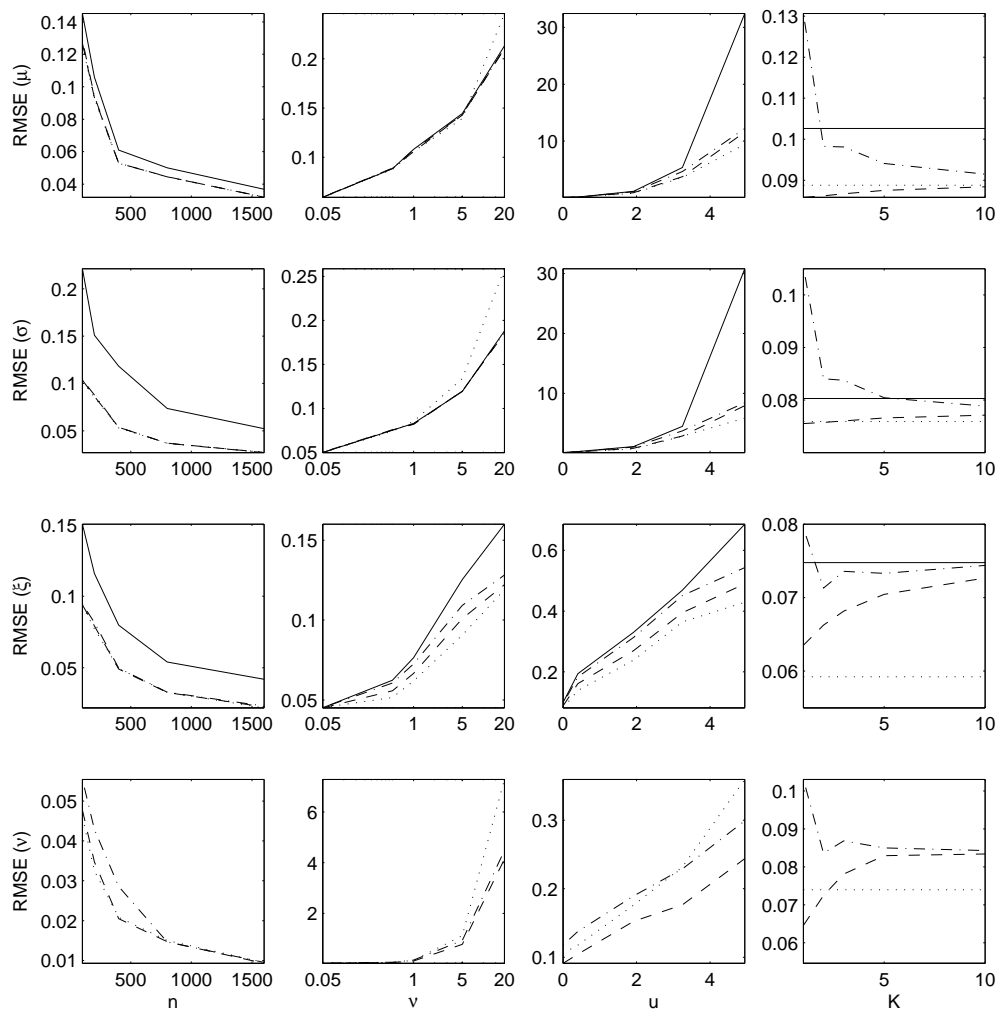


FIGURE 2. RMSE ( $y$ -axis) as a function of sample size  $n$  (first column), dependence parameter  $\nu$  (second column), threshold  $u$  (third column) and neighborhood size  $K$  (last column). Results obtained using 1000 simulations of a Gaussian extreme value process. Unless otherwise specified the time sampling is regular and the values  $\mu = 0$ ,  $\sigma = 1$ ,  $\xi = 0.3$ ,  $\nu = 0.5$ ,  $u = -\infty$  and  $n = 300$  were used. Solid line: MILE ; dotted line: MMLE ; dashed line:  $MPL_1E$  ; dashed-dotted line:  $MPL_5E$ . For the last column, the time step between successive observations is drawn from a uniform distribution on the interval  $(0, 2)$  and the dashed [resp. dashed-dotted] line corresponds to the  $MPL_K E$  with the first [resp. second] weighting strategy (see (13) [resp. (14)]).

- **AR(1)**:  $\{X_t\}$  is a discrete time stationary process which satisfies

$$X_t = \alpha X_{t-1} + \sqrt{1 - \alpha^2} \epsilon_t$$

for all  $t$ , where  $\alpha \in (-1, 1)$  describes the dependence between successive observations, and  $\{\epsilon_t\}$  is an iid sequence of a standard normal distribution. The marginal distribution of  $\{X_t\}$  is a standard normal distribution, and the extremal index (see [Coles \(2001\)](#)) is equal to one (no clustering of extremes). We use the value  $\alpha = 0.2$ .

- **logARMAX(1)**:  $\{X_t\}$  is a discrete time stationary process which satisfies  $X_t = \log(U_t)$ , where  $\{U_t\}$  is an ARMAX(1) process defined as

$$U_t = \max\{(1 - \alpha)U_{t-1}, \alpha \epsilon_t\}$$

for all  $t$ , where  $\alpha \in (0, 1)$  describes the dependence between successive observations and  $\{\epsilon_t\}$  is an iid sequence of a unit Fréchet distribution. The logarithmic transformation is used to avoid the numerical problems which occur when estimating quantities related to heavy tail distributions by simulation. The marginal distribution of  $\{U_t\}$  is unit Fréchet, whereas the one of  $\{X_t\}$  is Gumbel. The extremal index is  $\alpha$ . We use the value  $\alpha = 0.2$ .

- **OU** :  $\{X_t\}$  is a continuous time stationary process which satisfies

$$dX_t = -\alpha X_t dt + \sqrt{2\alpha} dW_t,$$

where  $\alpha > 0$  describes the dependence structure, and  $\{W_t\}$  is a standard Brownian motion. The marginal distribution of  $\{X_t\}$  is a standard normal distribution, and we retrieve the AR(1) model when the process is sampled at a regular time step. We use the value  $\alpha = 0.05$  in the sequel, and the time lags between successive observations are drawn from a uniform distribution on  $[0, 2]$ .

For each of these models, we first generate a long realization (equivalent to 1000 years with one observation per day) and fit a Gaussian extreme value process to the simulated sequence censored at the 95% quantile by computing the MPL<sub>1</sub>E. We then compare the following characteristics of the reference model and the fitted censored Gaussian extreme value process :

- mean number of up-crossings during a given time period (one year) as a function of the threshold;
- mean length of the sojourns above a varying threshold; and
- mean length of the sojourns below a varying threshold.

These quantities were selected because they summarize important properties of the extremal behavior of the processes and are important for practitioners. All quantities were computed using long simulations of both the original time series model (IID, AR(1), log-ARMAX(1) or OU generated using standard algorithms) and the fitted Gaussian extreme

value process. This is illustrated on Figure 3 which shows realizations of both the AR(1) model and the fitted Gaussian extreme value process, whereas the second column of Figure 4 permits a more systematic comparison of the extremal behavior of both processes. The fitted model is able to reproduce both the frequency of the up-crossings and the durations between successive up-crossings, even for high thresholds, but it slightly overestimates the mean length of the clusters above high thresholds. Indeed, for the AR(1) model, the mean length of the clusters tends to one when the threshold increases, as expected from the theory (no clustering of extremes), whereas the fitted Gaussian extreme value process exhibits small extremal dependence and thus clustering of extremes. Using a higher threshold for censoring before fitting the Gaussian extreme value process helps to improve these results and to retrieve extremal independence (not shown). According to the first column of Figure 4, the results are better for the IID model, which is a particular case of the AR(1) model with no dependence between successive observations. It is not surprising to obtain similar results for the OU (see the last column of Figure 4) and AR(1) models since they are equivalent when the time sampling is regular.

In contrast to the other models, the extreme values of the logARMAX(1) process tend to cluster. Figure 4 shows that the fitted model seems to be able to reproduce both the frequency of the up-crossings and the mean length of the clusters that tend to a limit greater than one, as expected from the theory. However, it seems to overestimate the mean length of the sojourns below high thresholds, although the erratic behavior of the curves suggests that the observed differences may be due to sampling error.

These simulation results indicate that the Gaussian extreme value process is able to capture important properties of the extremal behavior of several common time series models, and similar results were obtained for various other models we have tested (not reported).

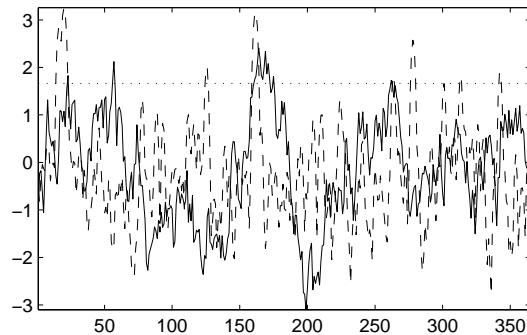


FIGURE 3. *Short samples of the AR(1) model (solid line) and fitted Gaussian extreme value process (dashed line). The horizontal dotted line is the threshold used for censoring.*

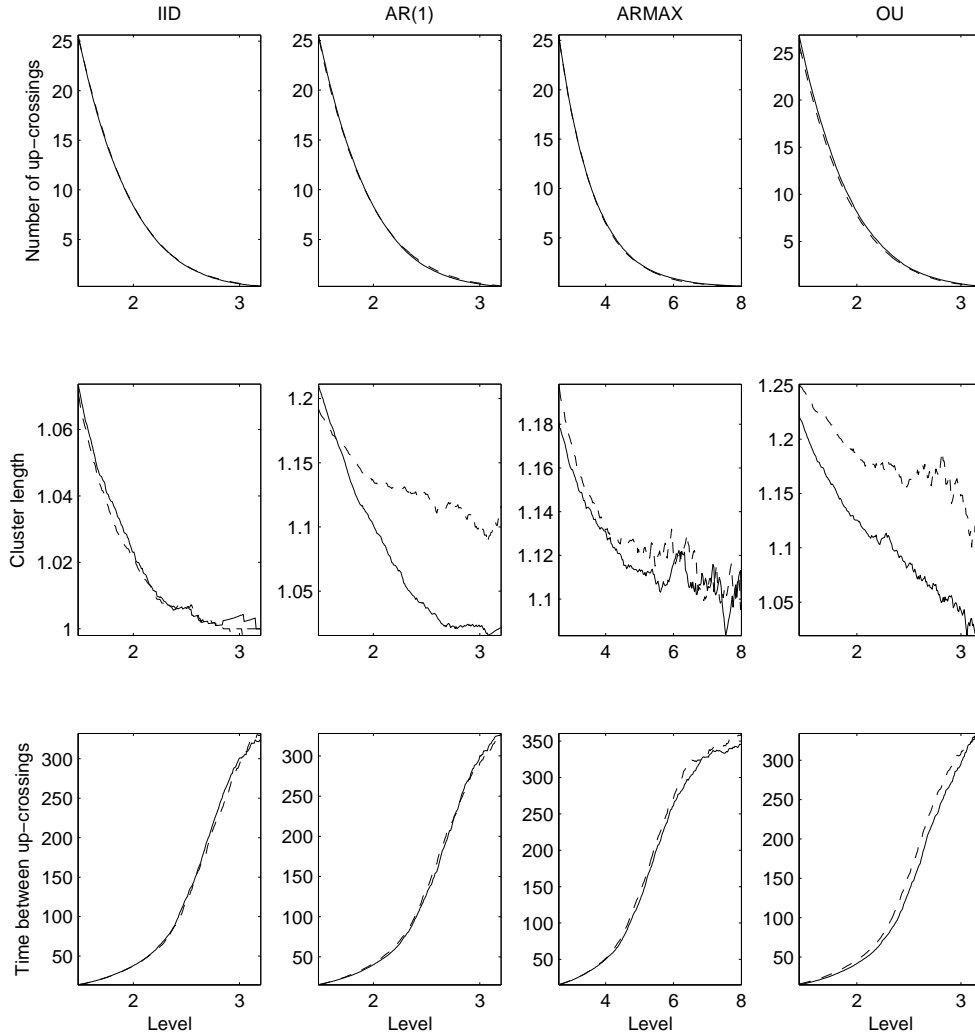


FIGURE 4. Comparison of the extremal behavior of classical processes (solid line) against the fitted Gaussian extreme value process (dashed line). From top row: mean number of up-crossings per year, mean length of clusters and mean time between consecutive up-crossings as a function of the threshold ( $x$ -axis). Results obtained by simulating 1000 years of each model (one observation per day).

4.2. *Simulation results in a realistic context for practical applications.* In this section, we validate our proposed methodology on shorter synthetic time series that better correspond to the amount of data typically available in environmental applications (i.e. a few years of data). For each of the time series models introduced in the previous section, we repeated the following numerical experiment 1000 times:



TABLE 1

Mean value of the estimated 100-year return level with 90% fluctuation intervals in parentheses. Simulation results based on 200 independent five-year synthetic sequences of each model. A declustering step was applied in the POT method (see [Coles \(2001\)](#)).

Method	IID	AR(1)	logARMAX(1)	OU
True value	4.03	4.03	8.90	3.79
POT	4.18 (3.12,6.02)	4.16 (3.14,5.68)	12.19 (5.31,29.96)	3.21 (2.31,5.04)
MMLE	3.89 (3.12,5.15)	3.90 (3.09,4.95)	18.77 (5.88,36.96)	3.62 (2.61,5.05)
CPL <sub>1</sub> E	3.84 (3.11,5.17)	3.76 (3.16,4.72)	9.52 (5.54,17.09)	3.62 (2.61,4.98)

- generate a five-year sequence (one observation per day) of the reference time series model;
- fit the censored Gaussian extreme value process to this sequence after censoring at the 95% quantile; and
- compute the 100-year return level for the fitted model which is defined as the level at which the mean number of **clusters** above this level in a 100-year time period is equal to one. This return level was chosen because it is generally the quantity of interest in practical applications. It depends on both the marginal distribution and the dependence structure of the process. It was computed by simulating a long realization (1000 years) of the fitted model.

It can be seen from Table 1 that the results obtained with the fitted censored Gaussian extreme value process clearly outperform those obtained with the usual POT method. The MMLE and CPL<sub>1</sub>E produce similar results for the three models with no extremal dependence (IID, AR(1) and OU) but those obtained with the CPL<sub>1</sub>E are clearly superior to those obtained with the MMLE in terms of accuracy and bias for the logARMAX(1) model. The IID and AR(1) models have almost the same 100-year return levels, which is expected from the theory since they have the same marginal distribution and no extremal dependence. The lower return period of the OU process, which also has the same marginal distribution and no extremal dependence when observed at a regular time step, may be due to the irregular time sampling. The extremal dependence of the logARMAX(1) model leads to a higher return level than the other models, but also to bigger bias and variance in the estimators, which is in conformity with the simulation results reported in Section 3.2 (see Figure 2).

**5. Application to significant wave height.** Significant wave height ( $H_s$ ) is an important oceanographic parameter that is directly related to the energy of a sea state. It was originally defined as the mean height of the one-third highest waves, and was thought to give about the same value as an experienced seaman’s eyeball estimate of wave height. With the development of instruments producing more accurate measurements of sea surface elevation,  $H_s$  was redefined as four times the standard deviation of the sea surface elevation on a certain space-time domain where the sea state conditions can be assumed

to be stationary. The ratio of four was chosen to ensure that the two definitions roughly coincide.

Offshore structures in particular must be designed to exceed a specific level of reliability, which is typically expressed in terms of return periods of  $H_s$ . The three sources of data (buoy, reanalysis and satellite) which can be used to estimate the extremal behavior of  $H_s$  are introduced in Section 5.1. In Section 5.2, we focus on a specific location in which buoy data are available and compare the results obtained with the three datasets. The buoy and satellite data give similar results, whereas the reanalysis data lead to significantly different results. Since the buoy is generally considered to be the reference, it suggests the use of satellite data when no buoy data are available at the location of interest. This is further discussed in Section 5.3 which shows maps of  $H_s$  return-periods in the North Atlantic based on satellite data.

5.1. *H<sub>s</sub> data.* The data used in this work come from the three sources briefly described below.

- **Reanalysis data.** The ERA-interim dataset is a global reanalysis carried out by the European Center for Medium-Range Weather Forecasts (ECMWF). It can be freely downloaded and used for scientific purposes.<sup>1</sup> In this work, we consider 21 years of data, from 1989 until 2009.
- **Buoy data.** We focus on data from the buoy Brittany (station 62163<sup>2</sup>), which is part of the UK Met Office monitoring network. It is located at position (47.5 N, 8.5 W) and provides hourly  $H_s$  data. In this work, we consider 10 years of data, from 1995 until 2005 (no data are available for 2000). Missing values represent about 7.7% of the data and are generally associated with extreme events (as breakdowns generally occur during storms), which is an important issue when implementing block maxima or POT approaches.
- **Satellite data.** The observations consist of  $H_s$  measured at discrete locations along one-dimensional tracks from seven different satellite altimeters which have been deployed progressively since 1991. The dataset and related information can be freely downloaded.<sup>3</sup> In this study, we consider data from 1992 until 2007.

A typical example of data coverage over a 24-hour time window in the North Atlantic Ocean can be seen in Figure 1. The reanalysis data are sampled over a regular  $1.5 \times 1.5$ -degree grid at synoptic times every six hours starting at midnight, in contrast to the irregular space-time sampling provided by the satellite altimeter. However, the reanalysis data tend to underestimate  $H_s$  variability (see the next section) and they provide information only at a synoptic scale, whereas satellite data give smaller-scale information as well.

---

<sup>1</sup><http://data.ecmwf.int/data/>

<sup>2</sup>[http://www.ndbc.noaa.gov/station\\_page.php?station=62163](http://www.ndbc.noaa.gov/station_page.php?station=62163)

<sup>3</sup><ftp://ftp.ifremer.fr/ifremer/cersat/products/swath/altimeters/waves/>

Buoys provide accurate information on sea-state conditions but are sparsely distributed over the ocean, and there is generally no buoy at the location of interest for a particular application. In such a situation, it is important to be able to derive estimates of the extremal behavior of  $H_s$  from the other sources of data introduced in this section, which are available all over the oceans. These datasets have been considered in numerous studies interested in the distributional properties of  $H_s$  (see e.g. [Challenor, Foale and Webb \(1990\)](#); [Tournadre and Ezraty \(1990\)](#); [Caires and Sterl \(2005\)](#); [Menéndez et al. \(2008\)](#); [Vinoth and Young \(2011\)](#)).

5.2. *Single-site analysis.* In this section, we focus on the location of the buoy Brittany and illustrate how the methodology introduced in this work can be used to estimate the extremal behavior of  $H_s$  at this location using the three datasets introduced in the previous section.

$H_s$  data are non-stationary with an important seasonal component. A classical approach to treating seasonality in meteorological applications is to block the data by month and fit a separate model each month, assuming that the different realizations of the same month across years are independent realizations of a common stochastic process. We adopt this approach herein, focusing on the month of December. Blocking the data by month leads however to waste data and probably to the loss of important information on extreme events. The development of non-stationary models which include seasonal and inter-annual components to cover the whole time series would be a valuable topic for future research.

Reanalysis and satellite data provide observations that are not exactly at the location of interest. Interpolation methods could be used, but may smooth the data (see [Ailliot et al. \(2011\)](#)). We thus decided to consider:

- the reanalysis data available at location (48 N, 9 W), which is the closest grid point to the buoy Brittany, and
- the time series obtained by retaining all of the closest observations to the buoy in the satellite tracks which intersect a  $3^\circ \times 3^\circ$  box centered on the location of interest (see [Vinoth and Young \(2011\)](#); [Wimmer, Challenor and Retzler \(2006\)](#)).

Figure 5 shows the resulting reanalysis time series, which exhibits an important inter-annual variability particularly when we look at the extreme values. There were two severe storms in which  $H_s$  exceeded 12 meters in 1989 and 2007, whereas for the other years  $H_s$  was always below 9 meters. These two storms exert a strong influence on the results obtained from fitting a model to extreme events. To facilitate comparison with the buoy data (which are unavailable for 1989 and 2007) we also consider a subset of reanalysis data for the years for which buoy data are available (see Figure 5). This dataset is referred to as "restricted reanalysis data" whereas the full reanalysis time series is named "full reanalysis data."

Figure 6 shows all of the data available for December 2005. The agreement between the reanalysis and buoy time series is generally good, although the reanalysis data tend to be

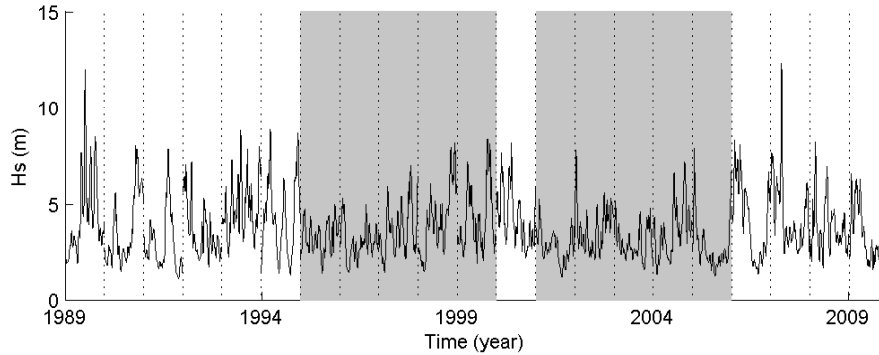


FIGURE 5. Reanalysis data for 21 months of December. The dotted vertical lines correspond to the beginning of the monthly blocks (1st of December of each year) and the gray area corresponds to the years in which both buoy and restricted reanalysis data are available.

smoother and to exhibit lower extremes, as confirmed by the quantile-quantile (QQ) plots in Figure 7, which show the buoy data to have higher quantiles than the restricted reanalysis data. However this no longer holds true when we compare the quantiles of the buoy and full reanalysis data because of the significant inter-annual variability (the months of December when the buoy data are available correspond to years with generally low  $H_s$ ). Finally, Figure 7 shows good agreement between the empirical quantiles of the buoy and satellite data which suggests that the satellite data may constitute a better source of information on high  $H_s$  than the reanalysis data. Figure 6 presents the complex temporal sampling of the satellite data with clusters of several observations and long gaps with no observation, which prevents the use of the standard methods of the extreme value theory (i.e. block maxima and POT).

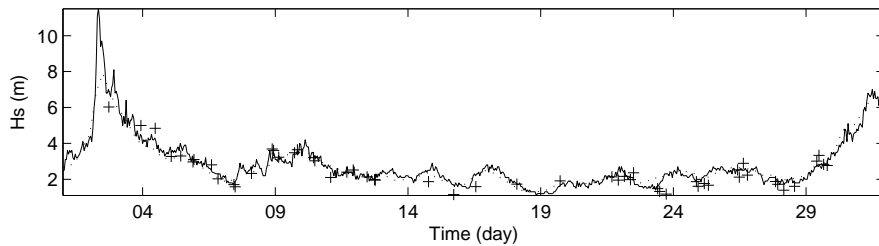


FIGURE 6. Comparison of the three time series for December 2005. Solid line: buoy data (location  $[47.5\text{ N}, 8.5\text{ W}]$ ); dotted line: reanalysis data (location  $[48\text{ N}, 9\text{ W}]$ ); plus points: closest satellite observation to the buoy from each satellite track within a  $3^\circ$  box.

We first focus on buoy data since this dataset is generally considered to be the reference for the other datasets (see e.g. Queffelec (2004)). The first step is to choose a censoring

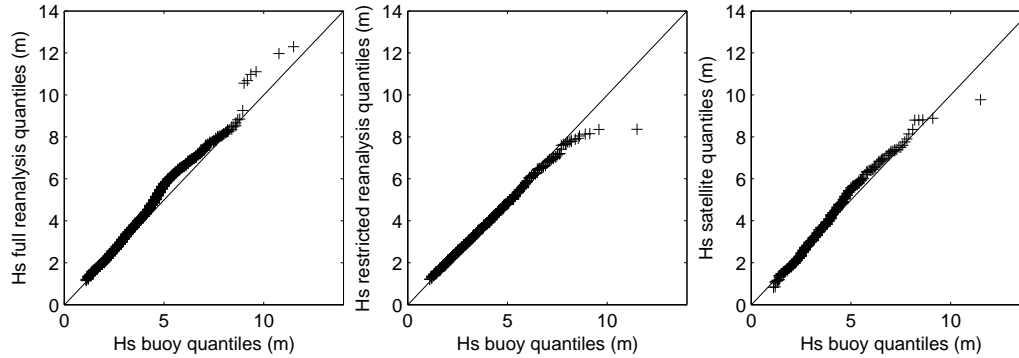


FIGURE 7. *QQ-plots of the empirical distribution of the buoy (x-axis) against the empirical distribution of the full reanalysis data (y-axis on the left panel), the reduced reanalysis data (y-axis on the middle panel) and the satellite data (y-axis on the right panel)*

threshold  $u$ . This is a crucial step since  $u$  must be high enough to justify approximation by probabilistic models derived from extreme value theory but not too high in order to keep enough observations to fit the model. A common tool for selecting an appropriate threshold is to fit the model for various thresholds and choose the lowest one that ensures the estimates are almost stable for any higher threshold value. Indeed, from a theoretical point of view, if the fitted censored Gaussian extreme value process is an appropriate model for describing the behavior of the observed process above a threshold  $u$ , then it should also be appropriate above a higher threshold. However, in practice, it is generally difficult to come up with a decision using such diagnostic plots. Figure 8 shows that the estimate of  $\nu$  seems to stabilize only over the threshold  $u = 8$  meters, which has been selected in the sequel. This threshold roughly corresponds to the 99% quantile of the marginal distribution.

The parameter values are given in Table 2 together with 95% confidence intervals computed using parametric bootstrap. The shape parameter  $\xi$  is slightly negative (bounded tail) but the sampling distribution shown in Figure 9 indicates that the difference with zero (Gumbel distribution) is not significant. This is in agreement with previous studies (see e.g. Caires and Sterl (2005)) in which  $\xi$  is often fixed to be equal to zero. More generally, Figure 9 shows the empirical distribution of the parameters obtained using parametric bootstrap and the strong relations between the estimates of the parameters  $\mu$ ,  $\sigma$  and  $\xi$ . High values for position parameter  $\mu$  are generally associated with high values for shape parameter  $\xi$ , which is compensated for by low values for scale parameter  $\sigma$ . As a consequence, any error on one parameter influences the value of the others, leading to wide confidence intervals for  $\mu$ ,  $\sigma$  and  $\xi$  (see Table 2). Parameter  $\nu$  is less correlated with the other parameters, although there is a noticeable positive correlation with  $\xi$ . In practical applications, the end user is generally interested in return levels, which are functions of the four parameters of the model, and thus the errors made on individual parameters may compensate for one another (see also Ribereau, Naveau and Guillou (2011)).

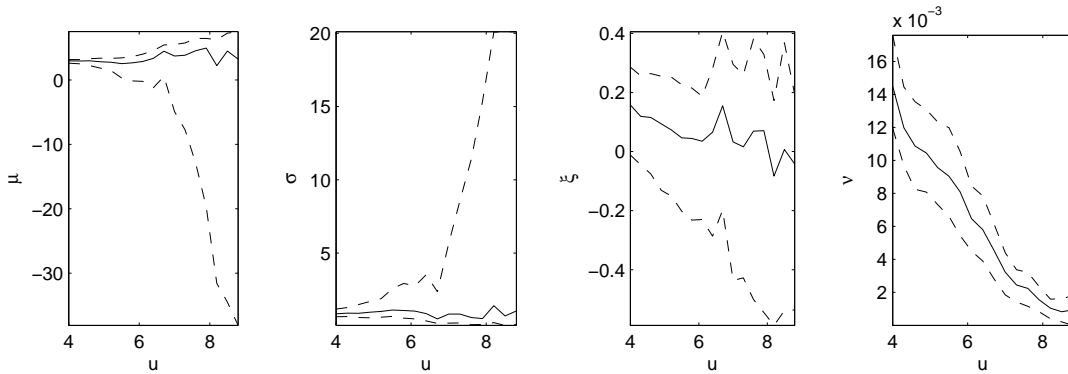


FIGURE 8. Values of the  $MPL_1E$  computed on buoy data as a function of threshold  $u$  ( $x$ -axis). From the left to right panels: estimates of  $\mu$ ,  $\sigma$ ,  $\xi$  and  $\nu$ . The dashed lines correspond to 95% confidence intervals computed using parametric bootstrap (results based on 1000 independent replications of the fitted model simulated with the temporal sampling of the original data).

Figure 10 compares various important characteristics of the extremal behavior of the data with those of the fitted model. The statistics computed from the data always lie in the 95% prediction intervals for the fitted model and thus the model seems to be able to reproduce both the marginal distribution and the dynamics of the observed time series above the selected threshold. This gives us confidence in the results obtained when extrapolating the extremal behavior of the data using the model. Using a lower threshold  $u$  leads to estimates with smaller variances (see Figure 8), but the fitted models are no longer able to reproduce the characteristics of the data above high levels (results not shown).

The censored Gaussian extreme value process was also fitted to the reanalysis and satellite data. For these datasets, we selected a lower threshold  $u = 6$  meters. This choice was based on the same diagnostic plots as those previously discussed for buoy data and practical considerations (using the threshold  $u = 8$  meters would lead to retaining fewer than 10 observations above the threshold for the satellite and restricted reanalysis data). The parameter values of the models fitted on the buoy and satellite time series are broadly similar (see Table 2) but exhibit important differences with those obtained on the two reanalysis datasets. In particular, parameter  $\nu$ , which describes the dynamics of the process, is higher for the reanalysis datasets. This is in agreement with Figure 6, which shows that the reanalysis data tend to be smoother than the buoy data. The value of  $\xi$  is close to zero for the buoy and satellite data, whereas it is significantly negative (bounded tail) for the restricted reanalysis data and slightly positive for the full reanalysis data, probably because of the influence of the two severe storms in 1989 and 2007 (see Figure 5). These results are also in agreement with Figure 7, which indicates that the full reanalysis dataset has a heavier tail than the buoy dataset, whereas the restricted reanalysis dataset has a lighter tail.

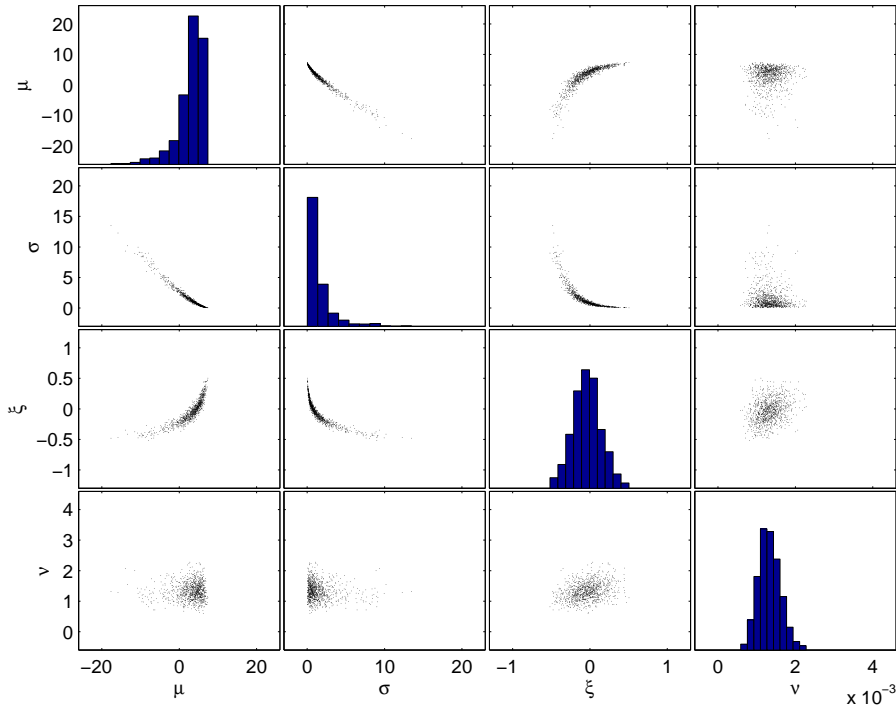


FIGURE 9. Empirical distribution of the parameters obtained using parametric bootstrap and the model fitted to buoy data. From the left to right panels: estimates of  $\mu$ ,  $\sigma$ ,  $\xi$  and  $\nu$ . The diagonal plots show a histogram of the marginal distribution and the other plots are scatter plots of the bivariate distributions (results based on 1000 independent replications of the fitted model simulated with the temporal sampling of the original data).

5.3. *Spatial analysis.* Similar results were obtained at the other locations for which buoy data were available. The buoy and satellite data generally lead to the identification of similar models, whereas the reanalysis data identify more extremal dependence and longer storms. If we believe the buoy data to be a good reference, then these results suggest that satellites may provide more accurate information on the extremal behavior of Hs than reanalysis data. In this context, the proposed methodology can be an efficient tool for estimating the extremal properties of Hs at any ocean location for which satellite data are available.

This is illustrated in Figure 11, which shows 20-year return levels in the North Atlantic computed using satellite data. To reduce the variability of the estimates, we have fixed the tail parameter  $\xi$  to be equal to zero which is a common assumption when fitting extreme value models to Hs data (see e.g. [Caires and Sterl \(2005\)](#)) and is in agreement with our previous single-site analysis. The map in Figure 11 exhibits a clear spatial structure, coherent with that obtained using another method in [Wimmer, Challenor and Retzler](#)

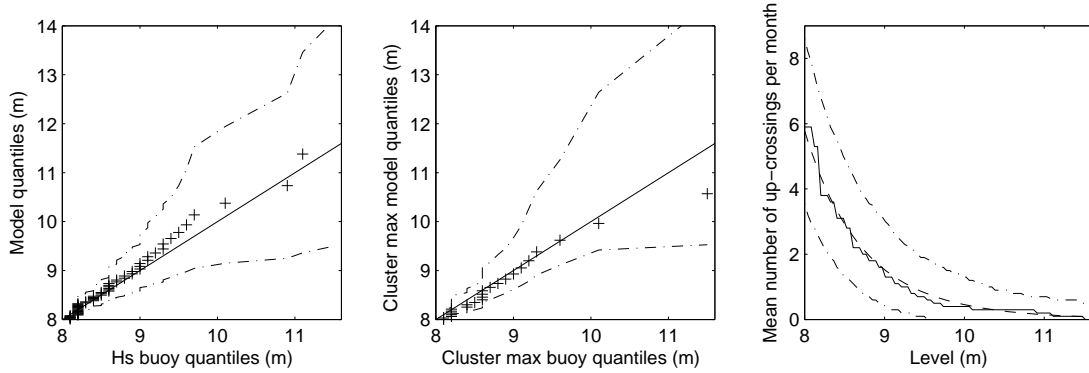


FIGURE 10. Comparison of the extremal behavior of the buoy data and fitted model. First panel: QQ-plot of the marginal distribution of the buoy ( $x$ -axis) against the fitted model. Second panel: QQ-plot of the cluster maxima of the buoy ( $x$ -axis) against the fitted model ( $y$ -axis). Third panel: mean number of up-crossings per month as a function of the level ( $x$ -axis) for the buoy data (solid line) and fitted model (dashed line). The dashed-dotted lines represent 95% prediction intervals computed by simulation (results based on 1000 independent replications of the fitted model simulated with the temporal sampling of the original data).

(2006). Further improvements may be obtained by constraining the parameters so that they vary smoothly in space (see e.g. Cooley, Nychka and Naveau (2007); Reich and Shaby (2012)), although such a sophisticated development is beyond the scope of this study.

**6. Conclusion.** In this paper, we propose an original method for analyzing the extremal behavior of univariate time series. Our approach is motivated by the need to analyze environmental time series with missing values or irregular sampling. Tests performed on classical time series models indicate that the proposed method also performs well on time series with regular sampling compared to the other methods which have been proposed in the literature. The parameters are estimated using a composite likelihood method, and both theoretical and simulation results indicate that doing so leads to consistent estimates. The results obtained on Hs data indicate that the proposed methodology can be used to estimate the extremal behavior of Hs from satellite data and produce accurate climatology of extreme Hs all over the ocean.

We believe our methodology to be sufficiently flexible to build extensions useful for practical applications. For example, it could deal with other max-stable processes, include non-stationary components or be extended to a space-time model. These possible extensions will be the subject of future research.

**Acknowledgments.** The authors are indebted to the Laboratoire d’Océanographie Spatiale, IFREMER and to the ECMWF for providing the data used in this study. We are also grateful to the anonymous reviewer, associate editor and editor for their constructive comments and suggestions, which have led to significant improvements to the paper.



TABLE 2

Thresholds, parameter values and return levels for the different datasets. 95% confidence intervals computed using parametric bootstrap are given in parentheses (results based on 1000 independent replications of the fitted models simulated with the temporal samplings of the original data).

	Full reanalysis	Restricted reanalysis	Buoy	Satellite
Threshold				
$u$	6	6	8	6
Nb obs $> u$	182	74	59	48
Parameter values				
$\mu$	4.20 (3.20,4.66)	2.19 (-6.85,3.80)	5.12 (-7.3,6.67)	3.80 (2.23,4.47)
$\sigma$	0.69 (0.41,1.31)	1.70 (0.81,8.83)	0.50 (0.11,7.23)	1.33 (0.86,2.69)
$\xi$	0.14 (-0.10,0.3)	-0.17 (-0.6,-0.02)	0.07 (-0.40,0.32)	0.01 (-0.25,0.17)
$\nu$	0.13 (0.10,0.17)	0.12 (0.07,0.18)	1e-3 (8e-4,2e-3)	0.05 (0.03,0.08)
Return levels				
$q_{10}$	10.1 (8.5,12.3)	8.2 (7.3,9.1)	10.4 (9.3,12.2)	12.1 (10.7,14.6)
$q_{20}$	11.0 (9.0,14.3)	8.5 (7.5,9.6)	10.8 (9.4,13.8)	12.9 (11.1,16.4)
$q_{50}$	12.5 (9.5,17.9)	8.8 (7.6,10.1)	11.4 (9.6,16.0)	14.0 (11.5,19.1)
$q_{100}$	13.6 (9.9,21.6)	9.0 (7.7,10.6)	11.8 (9.7,18.8)	14.7 (11.7,21.6)

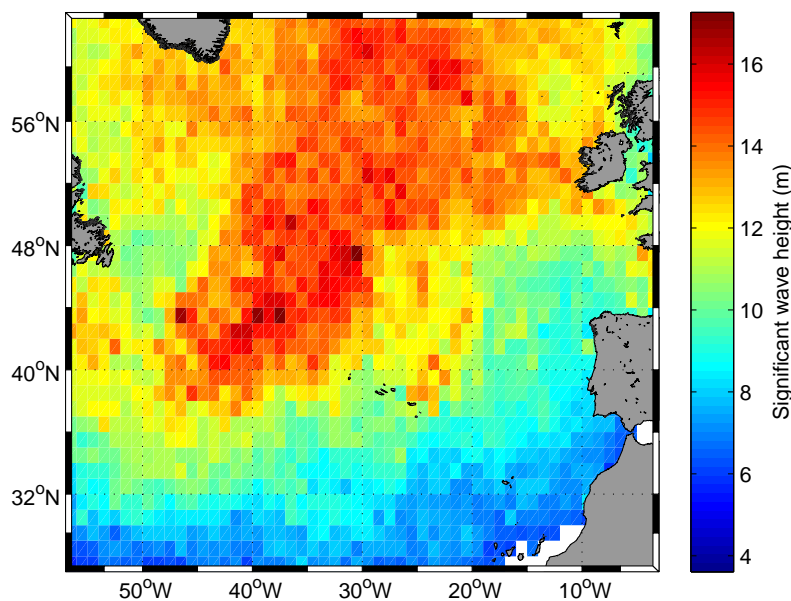


FIGURE 11. Map of 20-year return levels in the North Atlantic Ocean. A  $3^\circ$ -wide moving window was used to build the time series at the different locations by retaining the value closest to the center for each satellite track crossing the window. A variable threshold corresponding to the 95% quantile was used.

## SUPPLEMENTARY MATERIAL

**Supplementary material: Proof of the consistency of the  $MPL_1E$  estimates.**  
(doi: [COMPLETED BY THE TYPESETTER](#); .pdf). In the attached supplemental mate-

rial (Raillard, Ailliot and Yao (2013)), we prove the consistency of the  $MPL_1E$  estimator in an idealized situation with no censoring and known marginal distributions.

## References.

- AILLIOT, P., THOMPSON, C. and THOMSON, P. (2011). Mixed methods for fitting the GEV distribution. *Water Resources Research* **47** W05551.
- AILLIOT, P., BAXEVANI, A., CUZOL, A., MONBET, V. and RAILLARD, N. (2011). Space-time models for moving fields with an application to significant wave height fields. *Environmetrics* **22** 354–369.
- BEIRLANT, J., GOEGBEUR, Y., SEGERS, J. and TEUGELS, J. (2004). *Statistics of Extremes: Theory and Applications*. Hoboken, NJ: John Wiley & Sons.
- BENTON, D. and KRISHNAMOORTHY, K. (2002). Performance of the parametric bootstrap method in small sample interval estimates. *Advances and Applications in Statistics* **2** 269–285.
- BORTOT, P. and GAETAN, C. (2013). A latent process model for temporal extremes. *Scandinavian Journal of Statistics* n/a–n/a.
- CAIRES, S. and STERL, A. (2005). 100-year return value estimates for ocean wind speed and significant wave height from the ERA-40 data. *Journal of Climate* **18** 1032–1048.
- CHALLENGER, P. G., FOALE, S. and WEBB, D. J. (1990). Seasonal changes in the global wave climate measured by the Geosat altimeter. *International Journal of Remote Sensing* **11** 2205–2213.
- COLES, S. G. (2001). *An Introduction to Statistical Modeling of Extreme Values*. Springer Series in Statistics. Springer-Verlag London Ltd., London. [MR1932132](#)
- COOLEY, D., NYCHKA, D. and NAVEAU, P. (2007). Bayesian spatial modeling of extreme precipitation return levels. *Journal of the American Statistical Association* **102** 824–840. [MR2411647](#)
- COX, D. R. (2004). A note on pseudolikelihood constructed from marginal densities. *Biometrika* **92** 729–737.
- DAVISON, A. C. and SMITH, R. L. (1990). Models for exceedances over high thresholds. *Journal of the Royal Statistical Society Series B* **52** 393–442. [MR1086795 \(91k:62048\)](#)
- DE HAAN, L. (1984). A spectral representation for max-stable processes. *Annals of Statistics* **12** 1194–1204. [MR757776 \(86b:60089\)](#)
- DE HAAN, L. D. L. and FERREIRA, A. (2006). *Extreme Value Theory: An Introduction*. Springer Series in Operations Research and Financial Engineering. Springer, New York. [MR2234156 \(2007g:62008\)](#)
- DOS SANTOS, S. and LOPES, H. F. (2008). Copula, marginal distributions and model selection: A Bayesian note. *Statistics and Computing* **18** 313–320.
- DREES, H., DE HAAN L. and LI, D. (2006). Approximations to the tail empirical distribution function with application to testing extreme value conditions. *Journal of Statistical Planning and Inference* **136** 3498–3538.
- EMBRECHTS, P., KLÜPPELBERG, C. and MIKOSCH, T. (1997). *Modelling Extremal Events: For Insurance and Finance*. Applications of Mathematics **33**. Springer-Verlag, Berlin. [MR1458613 \(98k:60080\)](#)
- FAWCETT, L. and WALSHAW, D. (2007). Improved estimation for temporally clustered extremes. *Environmetrics* **18** 173–188. [MR2345653](#)
- FAWCETT, L. and WALSHAW, D. (2012). Estimating return levels from serially dependent extremes. *Environmetrics* **23** 272–283.
- FISHER, R. A. and TIPPETT, L. H. C. (1928). Limiting forms of the frequency distribution of the largest or smallest member of a sample. *Mathematical Proceedings of the Cambridge Philosophical Society* **24** 180–190.
- HUSER, R. and DAVISON, A. C. (In press). Space-time modelling of extreme events. *Journal of the Royal Statistical Society: Series B (Statistical Methodology)*.
- JEON, S. and SMITH, R. L. (2012). Dependence structure of spatial extremes using threshold approach. *arXiv preprint arXiv:1209.6344*.

- LEADBETTER, M. R., LINDGREN, G. and ROOTZÉN, H. (1983). *Extremes and Related Properties of Random Sequences and Processes*. Springer Series in Statistics. Springer-Verlag, New York. [MR691492 \(84h:60050\)](#)
- LINDSAY, B. G. (1988). Composite likelihood methods. Statistical inference from stochastic processes, Proc. AMS-IMS-SIAM Jt. Summer Res. Conf., Ithaca/NY 1987, Contemp. Math. 80, 221-239 (1988).
- MENÉNDEZ, M., MÉNDEZ, F. J., LOSADA, I. J. and GRAHAM, N. E. (2008). Variability of extreme wave heights in the northeast Pacific Ocean based on buoy measurements. *Geophysical Research Letters* **35** L22607.
- PADOAN, S. A., RIBATET, M. and SISSON, S. A. (2010). Likelihood-based inference for max-stable processes. *Journal of the American Statistical Association* **105** 263–277.
- QUEFFEULOU, P. (2004). Long-term validation of wave height measurements from altimeters. *Marine Geodesy* **27** 495–510.
- RAILLARD, N., AILLIOT, P. and YAO, J. (2013). Supplement to "Modeling extreme values of processes observed at irregular time step. Application to significant wave height."
- REICH, B. J. and SHABY, B. A. (2012). A hierarchical max-stable spatial model for extreme precipitation. *The Annals of Applied Statistics* **6** 1430–1451.
- REICH, B. J., SHABY, B. A. and COOLEY, D. (2013). A hierarchical model for serially-dependent extremes: A study of heat waves in the western US. *Journal of Agricultural, Biological, and Environmental Statistics* **In press** 1–17.
- RIBATET, M., OUARDA, T. B. M. J., SAUQUET, E. and GRESILLON, J. M. (2009). Modeling all exceedances above a threshold using an extremal dependence structure: Inferences on several flood characteristics. *Water Resources Research* **45** W03407.
- RIBEREAU, P., NAVEAU, P. and GUILLOU, A. (2011). A note of caution when interpreting parameters of the distribution of excesses. *Advances in Water Resources* **34** 1215–1221.
- SCHLATHER, M. (2002). Models for stationary max-stable random fields. *Extremes* **5** 33–44. [MR1947786 \(2003k:60115\)](#)
- SMITH, R. L. (1990). Max-stable processes and spatial extremes. Unpublished.
- SMITH, R. L., TAWN, J. A. and COLES, S. G. (1997). Markov chain models for threshold exceedances. *Biometrika* **84** 249–268. [MR1467045 \(98f:62271\)](#)
- TOURNADRE, J. and EZRATY, R. (1990). Local climatology of wind and sea state by means of satellite radar altimeter measurements. *Journal of Geophysical Research* **95** 18255–18268.
- VARIN, C. (2008). On composite marginal likelihoods. *Advances in Statistical Analysis* **92** 1–28. [MR2414624](#)
- VARIN, C. and VIDONI, P. (2005). A note on composite likelihood inference and model selection. *Biometrika* **92** 519–528. [MR2202643](#)
- VINOTH, J. and YOUNG, I. R. (2011). Global estimates of extreme wind speed and wave height. *Journal of Climate* **24** 1647–1665.
- WIMMER, W., CHALLENGER, P. and RETZLER, C. (2006). Extreme wave heights in the North Atlantic from altimeter data. *Renewable Energy* **31** 241–248.

**MODELING EXTREME VALUES OF PROCESSES OBSERVED AT  
IRREGULAR TIME STEPS: APPLICATION TO SIGNIFICANT WAVE  
HEIGHT.  
SUPPLEMENTARY MATERIAL**

BY NICOLAS RAILLARD\*

*Laboratoire de Mathématiques de Bretagne Atlantique, UMR 6205, Université de Brest  
Laboratoire d'Océanographie Spatiale, IFREMER  
Insititut de Recherche Mathématique de Rennes, UMR 6625, Université de Rennes 1*

BY PIERRE AILLIOT

*Laboratoire de Mathématiques de Bretagne Atlantique, UMR 6205, Université de Brest  
AND*

BY JIANFENG YAO

*Department of Statistics & Actuarial Sciences, The University of Hong Kong*

**1. Consistency of  $MPL_1$  estimator.** In this supplementary material, we prove the following theorem.

**THEOREM 1.1.** *Let  $\{Z_t\}$  be a Gaussian extreme value process with unit Fréchet margins, as defined in the paper, and dependence parameter  $\nu^* \in \Theta = [\nu_-, \nu_+]$  with  $0 < \nu_- < \nu_+$ . Assume that the process is observed at regular time  $\{1..n\}$ , and denote*

$$L_n(\nu) = \prod_{i=1}^{n-1} \frac{\partial^2 F_Z}{\partial z_1 \partial z_2}(Z_i, Z_{i+1}; \nu),$$

*the pairwise likelihood function, with  $F_z$  defined by*

$$F_Z(z_{t_1}, z_{t_2}; \nu) = \mathbb{P}(Z_{t_1} \leq z_{t_1}, Z_{t_2} \leq z_{t_2}) = \exp[-V(z_{t_1}, z_{t_2}; \nu)],$$

*and*

$$(1) \quad V(z_{t_1}, z_{t_2}; \nu) = \frac{1}{z_{t_1}} \Phi \left( \frac{a}{2} + \frac{1}{a} \log \frac{z_{t_2}}{z_{t_1}} \right) + \frac{1}{z_{t_2}} \Phi \left( \frac{a}{2} + \frac{1}{a} \log \frac{z_{t_1}}{z_{t_2}} \right).$$

*We define last  $\hat{\nu}_n = \operatorname{argmax} L_n(\nu)$  as the corresponding estimator of  $\nu^*$ . Then,  $\hat{\nu}_n$  is a strongly consistent estimator of  $\nu^*$ , i.e.*

$$\lim_{n \rightarrow \infty} \hat{\nu}_n = \nu^* \text{ a.s.}$$

---

\*Corresponding Author (E-mail: nicolas.raillard@gmail.com)

A Gaussian extremal process  $\{Z_t\}$  is a moving maxima process as defined in [Stoev \(2008\)](#). Using the results given in that paper, we deduce that  $\{Z_t\}$  is a stationary unit Fréchet process, continuous in probability, mixing, and hence ergodic. It allows us to use the following theorem, which is a straightforward generalization of Theorem 1.12 in [Pfanzagl \(1969\)](#):

**THEOREM 1.2.** *Let  $\{Z_i\}_{i=1,\dots,n}$  be a stationary and ergodic process, whose distribution depends on a parameter  $\nu^* \in \Theta$ , where  $\Theta$  is a compact subset of  $\mathbb{R}$ , and let  $Q_n$  be a contrast function defined as*

$$Q_n(\nu) = \frac{1}{n} \sum_{i=1}^{n-1} f(Z_i, Z_{i+1}; \nu),$$

where  $f$  is a measurable function with real values and continuous in  $\nu$ . Suppose that:

- (a)  $\mathbb{E} \inf_{\nu \in \Theta} f(Z_1, Z_2; \nu) > -\infty$ ;
- (b)  $\nu \mapsto \mathbb{E} f(Z_1, Z_2; \nu)$  has a unique finite minimum at  $\nu^*$ .

Then, the minimum contrast estimator  $\hat{\nu}_n = \operatorname{argmin}_{\nu \in \Theta} Q_n(\nu)$  is strongly consistent:

$$\lim_{n \rightarrow \infty} \hat{\nu}_n = \nu^* \text{ a.s.}$$

We use this theorem with

$$f(Z_1, Z_2; \nu) = -\log p(Z_1, Z_2; \nu),$$

where  $p(z_1, z_2; \nu)$  denotes the joint pdf of  $(Z_1, Z_2)$ ,  $\Theta = (\nu_-, \nu_+)$  with  $0 < \nu_- < \nu_+$ . An explicit expression for  $f$  is given in Section 1.1. Properties (1) and (2) of Theorem 1.2 are verified in Sections 1.2 and 1.3, respectively.

1.1. *Expression of the contrast.* We have

$$p(Z_1, Z_2; \nu) = \frac{\partial^2}{\partial z_1 \partial z_2} F_Z(z_1, z_2; \nu),$$

with  $F_Z(z_1, z_2; \nu) = \exp(-V(z_1, z_2; \nu))$  and  $V$  defined in (1) and thus

$$f(Z_1, Z_2; \nu) = V(z_1, z_2; \nu) - \log \left( \frac{\partial V}{\partial z_1}(z_1, z_2) \frac{\partial V}{\partial z_2}(z_1, z_2) + \frac{\partial^2 V}{\partial z_1 \partial z_2}(z_1, z_2) \right).$$

Function  $V$  and its derivatives satisfy

$$\begin{aligned} V(z_1, z_2; \nu) &= \frac{\Phi(a/2 + 1/a \log \frac{z_2}{z_1})}{z_1} + \frac{\Phi(a/2 + 1/a \log \frac{z_1}{z_2})}{z_2} = \frac{\Phi(w)}{z_1} + \frac{\Phi(v)}{z_2}, \\ \frac{\partial V}{\partial z_1}(z_1, z_2; \nu) &= -\frac{\Phi(w)}{z_1^2} - \frac{\varphi(w)}{az_1^2} + \frac{\varphi(v)}{az_1 z_2}, \\ \frac{\partial V}{\partial z_2}(z_1, z_2; \nu) &= -\frac{\Phi(v)}{z_2^2} - \frac{\varphi(v)}{az_2^2} + \frac{\varphi(w)}{az_1 z_2}, \\ \frac{\partial^2 V}{\partial z_1 \partial z_2}(z_1, z_2; \nu) &= -\frac{v\varphi(w)}{a^2 z_1^2 z_2} - \frac{w\varphi(v)}{a^2 z_1 z_2^2}, \end{aligned}$$

with

$$\begin{aligned} w &= \frac{a}{2} + \frac{1}{a} \log \frac{z_2}{z_1}, \\ v &= a - w = \frac{a}{2} + \frac{1}{a} \log \frac{z_1}{z_2}, \\ \varphi(w) &= \frac{1}{\sqrt{2\pi}} e^{-a^2/8} e^{-\frac{\log^2(z_1/z_2)}{2a^2}} \sqrt{\frac{z_1}{z_2}}, \\ \varphi(v) &= \frac{1}{\sqrt{2\pi}} e^{-a^2/8} e^{-\frac{\log^2(z_1/z_2)}{2a^2}} \sqrt{\frac{z_2}{z_1}}. \end{aligned}$$

Taking into account that  $\frac{\varphi(w)}{az_1^2} - \frac{\varphi(v)}{az_1 z_2} = 0$ , the following simplified expressions for the derivatives of  $V$  are obtained:

$$\begin{aligned} \frac{\partial V}{\partial z_1}(z_1, z_2) &= -\frac{\Phi(w)}{z_1^2}, \\ \frac{\partial V}{\partial z_2}(z_1, z_2) &= -\frac{\Phi(v)}{z_2^2}, \\ \frac{\partial^2 V}{\partial z_1 \partial z_2}(z_1, z_2) &= -\frac{\varphi(w)}{az_1^2 z_2} = -\frac{\varphi(v)}{az_2^2 z_1} = \frac{e^{-a^2/8} \exp\left(\frac{\log^2 \frac{z_2}{z_1}}{2a^2}\right)}{(z_1 z_2)^{3/2}}. \end{aligned}$$

Finally, we deduce that

$$(2) \quad f(z_1, z_2; \nu) = V(z_1, z_2; \nu) - \log \left[ \frac{\Phi(w)\Phi(v)}{a^2 z_1 z_2} + \frac{\varphi(w)}{az_1^2 z_2} \right].$$

1.2. *Lower bound (a).* We have

$$\inf_{\nu} \{f(z_1, z_2; \nu)\} \geq \inf_{\nu} \{V(z_1, z_2; \nu)\} + \inf_{\nu} \left\{ -\log \left[ \frac{\Phi(w)\Phi(v)}{a^2 z_1 z_2} + \frac{\varphi(w)}{az_1^2 z_2} \right] \right\},$$

and each term of the right-hand side of this expression is treated separately below.

- **Term**  $V(z_1, z_2; \nu)$ .

$V$  can be bounded using the Fréchet bound (Fréchet (1951)),

$$P(Z_1 \leq z_1) + P(Z_2 \leq z_2) - 1 \leq \mathbb{P}(Z_1 \leq z_1, Z_2 \leq z_2) \leq \min\{P(Z_1 \leq z_1), P(Z_2 \leq z_2)\},$$

which implies that

$$\min\left(-\frac{1}{z_1}, -\frac{1}{z_2}\right) \leq V(z_1, z_2; \nu) \leq \exp\left(-\frac{1}{z_1}\right) + \exp\left(\frac{1}{z_2}\right),$$

and thus

$$\inf_{\nu} \{V(z_1, z_2; \nu)\} \geq \min\left(-\frac{1}{z_1}, -\frac{1}{z_2}\right).$$

The right-hand term of the last expression has a finite expectation since  $\frac{1}{Z_1}$  and  $\frac{1}{Z_2}$  have unit exponential distributions.

- **Term**  $-\log\left[\frac{\Phi(w)\Phi(v)}{a^2 z_1 z_2} + \frac{\varphi(w)}{a z_1^2 z_2}\right]$ .

We have

$$\begin{aligned} -\log\left[\frac{\Phi(w)\Phi(v)}{z_1 z_2} \nu^2 + \frac{\varphi(w)}{z_1^2 z_2} \nu\right] &\geq 1 - \frac{\Phi(w)\Phi(v)}{z_1 z_2} \nu^2 + \frac{\varphi(w)}{z_1^2 z_2} \nu \\ &\geq 1 - \frac{\nu^2}{z_1 z_2} \\ &\geq 1 - \frac{\nu_+^2}{z_1 z_2}, \end{aligned}$$

and Cauchy's inequality implies that the right-hand term of the last expression has a finite expectation since

$$\mathbb{E}\left[\frac{1}{Z_1 Z_2}\right] \leq \sqrt{\mathbb{E}[1/Z_1^2] \mathbb{E}[1/Z_2^2]} = 1.$$

1.3. *Identifiability (b)*. We must now prove that  $\nu \mapsto \mathbb{E}f(Z_1, Z_2; \nu)$  has a unique finite minimum at  $\nu^*$  on  $\Theta = [\nu_- \nu_+]$ . To this end we denote by  $P_\nu$  the distribution with density function  $p(z_1, z_2; \nu)$ . Then,

$$\mathbb{E}_{\nu^*} \left[ -\log \frac{p(Z_1, Z_2; \nu)}{p(Z_1, Z_2; \nu^*)} \right] = K(P_{\nu^*}, P_\nu),$$

is the Kullback-Leibler divergence between  $P_{\nu^*}$  and  $P_\nu$ . We have  $K \geq 0$  and  $K = 0$  iff  $P_\nu = P_{\nu^*}$ . As the density functions are positive and continuous in  $(z_1, z_2)$ , this is equivalent

to  $p(z_1, z_2; \nu^*) = p(z_1, z_2; \nu)$  for all  $(z_1, z_2)$ . In particular,  $K = 0$  implies that for all  $z_1 = z_2 = z > 0$ , we have

$$\exp \left[ -\frac{2}{z} \Phi \left( \frac{1}{2\nu} \right) \right] \left[ \frac{\Phi \left( \frac{1}{2\nu} \right)^2}{z^2} \nu^2 + \frac{\varphi \left( \frac{1}{2\nu} \right)}{z^3} \nu \right] = \exp \left[ -\frac{2}{z} \Phi \left( \frac{1}{2\nu^*} \right) \right] \left[ \frac{\Phi \left( \frac{1}{2\nu^*} \right)^2}{z^2} \nu^{*2} + \frac{\varphi \left( \frac{1}{2\nu^*} \right)}{z^3} \nu^* \right].$$

Letting  $z \rightarrow 0$  while  $z > 0$  we can see that the exponents in the exponential function must be equal, i.e.

$$\Phi \left( \frac{1}{\nu} \right) = \Phi \left( \frac{1}{\nu^*} \right).$$

Hence,  $\nu = \nu^*$ . The proof is complete.

### References.

- FRÉCHET, M. (1951). Sur les tableaux de corrélation dont les marges sont données. *Annales de l'Université de Lyon* **14** 53–77. [MR0049518 \(14,189c\)](#)
- PFANZAGL, J. (1969). On the measurability and consistency of minimum contrast estimates. *Metrika* **14** 249–272.
- STOEV, S. A. (2008). On the ergodicity and mixing of max-stable processes. *Stochastic Processes and their Applications* **118** 1679–1705. [MR2442375 \(2009e:60116\)](#)